$S = \frac{1}{2}$ quantum critical spin ladders produced by orbital ordering in Ba_2CuTeO_6

A. S. Gibbs,[1,2,3,4,*] A. Yamamoto,[3] A. N. Yaresko,[1] K. S. Knight,[4] H. Yasuoka,[5] M. Majumder,[5] M. Baenitz,[5] P. J. Saines,[6] J. R. Hester,[7] D. Hashizume,[3] A. Kondo,[8] K. Kindo,[8] and H. Takagi[1,2,9]

[1]*Max Planck Institute for Solid State Research, Heisenbergstrasse 1, 70569 Stuttgart, Germany*
[2]*Department of Physics, The University of Tokyo, Hongo 7-3-1, Bunkyo-ku, Tokyo, 113-0033, Japan*
[3]*RIKEN Advanced Science Institute, 2-1 Hirosawa, Wako, Saitama 351-0198, Japan*
[4]*ISIS Facility, Rutherford Appleton Laboratory, Harwell Campus, Didcot, OX11 0QX, United Kingdom*
[5]*Max Planck Institute for Chemical Physics of Solids, Nöthnitzer Strasse 40, 01187 Dresden, Germany*
[6]*School of Physical Sciences, University of Kent, Canterbury, CT2 7NH, United Kingdom*
[7]*Australian Centre for Neutron Scattering, ANSTO, Locked Bag 2001, Kirrawee DC, NSW 2232, Australia*
[8]*Institute for Solid State Physics, The University of Tokyo, Kashiwa, Chiba 277-8581, Japan*
[9]*Institute for Functional Materials and Quantum Technologies, University of Stuttgart, Pfaffenwaldring 57, 70569 Stuttgart, Germany*

(Received 3 November 2015; revised manuscript received 7 February 2017; published 21 March 2017)

The ordered hexagonal perovskite Ba_2CuTeO_6 hosts weakly coupled $S = \frac{1}{2}$ spin ladders produced by an orbital ordering of Cu^{2+}. The magnetic susceptibility $\chi(T)$ of Ba_2CuTeO_6 is well described by that expected for isolated spin ladders with exchange coupling of $J \approx 86$ K but shows a deviation from the expected thermally activated behavior at low temperatures below $T^* \approx 25$ K. An anomaly in $\chi(T)$, indicative of magnetic ordering, is observed at $T_{mag} = 16$ K. No clear signature of long-range ordering, however, is captured so far in NMR $1/T_1$, specific heat or neutron diffraction measurements at and below T_{mag}. The marginal magnetic transition, indicative of strong quantum fluctuations, is evidence that Ba_2CuTeO_6 is in very close proximity to a quantum critical point between magnetically ordered and spin-gapped phases controlled by interladder couplings.

DOI: 10.1103/PhysRevB.95.104428

Spin ladder systems have proved to be a rich source of physics over the years. Isolated two-leg $S = \frac{1}{2}$ spin ladders are known to have a spin-gapped ground state, in which correlations decay with an exponential spatial dependence and with spin-1 excitations, when both the rung coupling J_r and leg coupling J_l are nonzero [1]. When couplings between the ladders (J_{inter}) are present the system is pushed towards long-range ordering. With increasing J_{inter}, a quantum critical point (QCP) appears at the onset of long-range ordering $J_{inter} = J_c$, as depicted in the schematic phase diagram shown in Fig. 1(a). This is the case for both 3D coupled ladders [2,3], a 2D planar array of ladders [2,4], and a 2D stacked array of ladders [5]. The critical interladder coupling is of the order $J_{inter}/J \approx 0.1$–0.4 when $J = J_l = J_r$ but the exact value depends not only on the geometry of interladder coupling but also the ratio of J_r/J_l and the additional interactions in the system.

Despite the presence of quantum criticality in ladders being well established theoretically, the experimental realization remains challenging. Very few materials have so far been found to be near to this QCP. Often the candidates turn out to be in the strong-leg limit, for example bis(2,3-dimethylpyridinium) tetrabromocuprate [6], or the strong-rung (dimer) limit such as $(C_5H_{12}N)_2CuBr_4$ [7] and CaV_2O_5 [8,9], which places those systems far from isotropic ladder physics. It is not easy to tune J_{inter} close to J_c. (Dimethylammonium)(3,5-dimethylpyridinium)$CuBr_4$ was shown to contain isotropic ladders with a strong antiferromagnetic interladder coupling $J_{inter}/J = 0.32$, placing it close to the QCP, and displays long-range magnetic ordering at 2 K [10,11]. The observation of a pronounced specific heat anomaly at the magnetic transition indicates that the interladder coupling is too strong to capture a clear signature of the criticality.

Ba_2CuTeO_6 with $S = \frac{1}{2}$ Cu^{2+} crystallizes in an ordered hexagonal perovskite structure [12,13]. As can be seen in Figs. 1(b) and 1(d), the crystal structure consists of alternate stacking along the c axis of layers with triangular arrangements of CuO_6 octahedra and layers with triangular arrangements of TeO_6 octahedra. The CuO_6 and TeO_6 octahedra in neighboring layers are connected alternately by their corners and faces, giving rise to the unit cell containing two Cu layers and two Te layers along the c axis. A uniform Jahn-Teller distortion of the CuO_6 octahedra [Fig. 1(b)] with Cu^{2+} occurs below $T_{J\text{-}T} \approx 850$ K, which leads to the emergence of ferro-orbital ordering of the $d_{x^2-y^2}$ orbitals [14]. This should make the magnetic coupling of the $S = \frac{1}{2}$ Cu^{2+} spins anisotropic. Hybridization of the $d_{x^2-y^2}$ orbitals with $2p$ orbitals of the four oxygen ions lying in the plane of the $d_{x^2-y^2}$ orbital, and hopping between O $2p$ orbitals are anticipated to be responsible for the leading superexchange process between the neighboring Cu^{2+} spins within the corner-sharing CuO_6-Te-CuO_6 layered unit [Figs. 1(b) and 1(c)]. Therefore, as shown in Fig. 1(c), the two couplings, J between the neighboring Cu^{2+} along the monoclinic b axis within the triangular plane and J' between the pairs of Cu^{2+} in adjacent Cu planes, should be dominant, which would give rise to the formation of $S = \frac{1}{2}$ ladders.

In this study we show that the magnetic susceptibility and NMR data on Ba_2CuTeO_6 are fully consistent with the presence of coupled $S = \frac{1}{2}$ ladders. The sizable interladder coupling places this compound almost exactly at the QCP. A marginal magnetic transition, lacking clear signatures of a transition in NMR, specific heat, and neutron diffraction data, was identified in the magnetic susceptibility $\chi(T)$ which we argue to mirror the presence of strong quantum fluctuations around the QCP.

*alexandra.gibbs@stfc.ac.uk

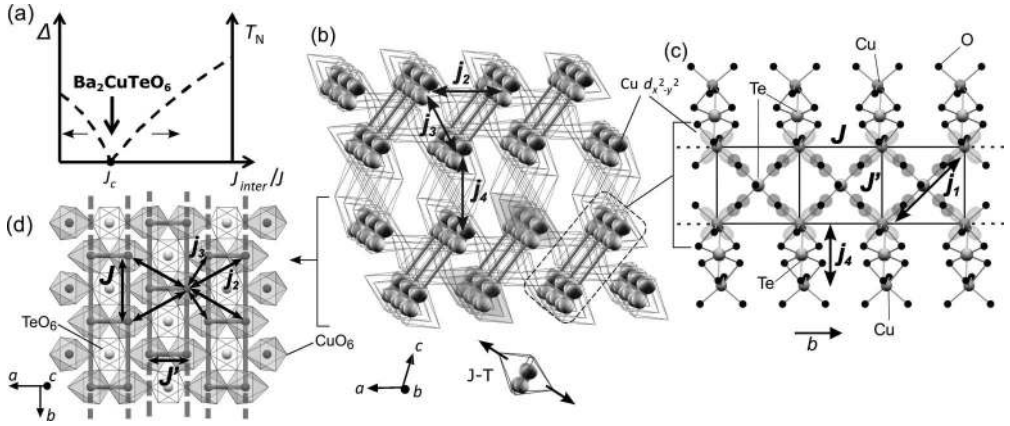

FIG. 1. (a) A rough schematic phase diagram at $T = 0$ for the two-leg $S = \frac{1}{2}$ antiferromagnetic ladder system with interladder coupling J_{inter}. The spin gap Δ is suppressed with increasing J_{inter} and goes to zero at the critical coupling J_c. For $J_{\text{inter}} > J_c$ long-range order is expected to develop below T_N. The arrow indicates a possible position for Ba_2CuTeO_6 in this phase diagram. (b) The chain and ladder arrangement in Ba_2CuTeO_6. The Cu^{2+} chains run along the monoclinic b axis (into the page) and form ladders between layers linked by corner-sharing TeO_6 octahedra (a single ladder is shaded and a second outlined). The ladders, indicated by thick gray lines, form a stacked layer within the ab plane. The interladder couplings are indicated by arrows. The inset with label "J-T" indicates the Jahn-Teller distortion direction. (c) The Cu^{2+} chains running along the b axis in Ba_2CuTeO_6. These chains can couple to form ladders via superexchange through oxygen ions. The intraladder leg and rung exchange couplings are indicated by J and J', respectively. The diagonal intraladder coupling is labeled j_1 and the intralayer interladder couplings are labeled j_2 and j_3. The interlayer coupling between ladders through face-sharing TeO_6 octahedra is labeled j_4. (d) A single layer of ladders in Ba_2CuTeO_6. J, J', j_2, and j_3 are indicated by arrows. The ladders are shown as thick gray lines.

Polycrystalline samples were prepared from stoichiometric mixtures of dried $BaCO_3$, CuO, and TeO_2 under flowing oxygen at 950–1000 °C. Powder x-ray diffraction and neutron diffraction on HRPD at ISIS [15,16] confirmed the samples to be of single phase. Single crystals were grown with a flux method based upon that of Köhl *et al.* [12,17] using $BaCO_3$, CuO, and TeO_2. Single crystal x-ray diffraction at $T = 296$ K confirmed the structure to be consistent with that reported by Köhl *et al.* [12] but in a higher symmetry space group of $C2/m$ [13]. In $\chi(T)$ for the single crystals and powders no Curie-like impurity contribution could be well fitted. A best estimate of the magnetic impurity content indicates <0.1% $S = \frac{1}{2}$ impurities, showing that our samples are extremely clean, partly due to full cation ordering caused by the contrasting ionic radii and valences of Cu^{2+} and Te^{6+}. Magnetization and specific heat were measured using a Quantum Design MPMS and PPMS, respectively. ^{125}Te NMR ($I = 1/2$ and about 7% natural abundance) measurements at a fixed frequency of 55.44 MHz (corresponding to $\mu_0 H = 4.12$ T) were performed for $2 \leqslant T \leqslant 300$ K using a conventional pulsed NMR technique.

Examination of the temperature dependence of $\chi(T)$, shown in Fig. 2, confirms the hypothesis of Ba_2CuTeO_6 as a quasi-1D ladder system. The broad overturn around $T \approx 75$ K is characteristic of low-dimensional systems. Fits to the inverse susceptibility for $170 \leqslant T \leqslant 300$ K gave $\theta_W \approx -113$ K indicating reasonably strong antiferromagnetic interactions and an effective moment of 1.96 μ_B/Cu^{2+}. $\chi(T)$ is not particularly well fitted by a Heisenberg chain model [18,19] but it is better described by an isolated two-leg ladder model [5] above $T = 35$ K as can be seen in Fig. 2 (expressions are given in the Supplemental Material (SM) [20]). The ladder model fit, including correction for core diamagnetism $\chi_{\text{dia}} = -1.48 \times$

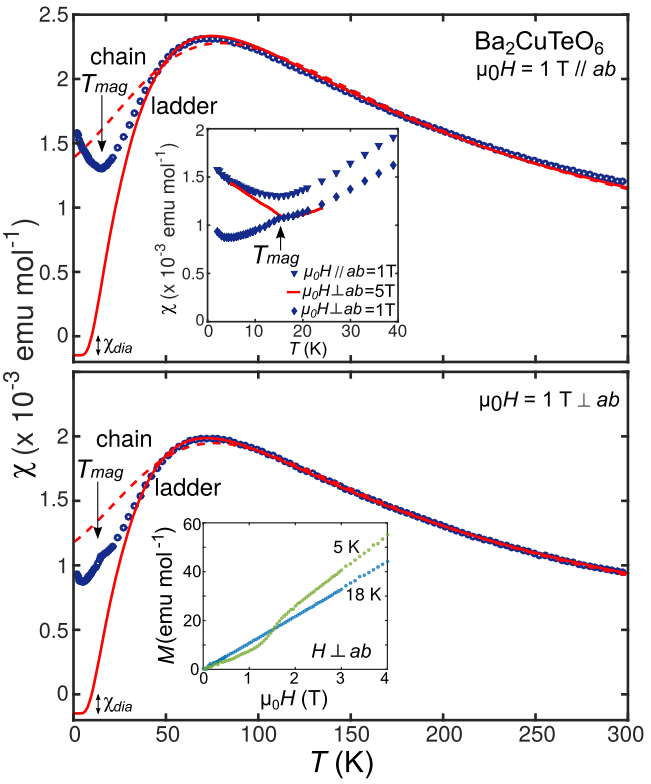

FIG. 2. $\chi(T)$ for Ba_2CuTeO_6 single crystal arrays with the magnetic field of $\mu_0 H = 1$ T applied parallel (upper panel) and perpendicular (lower panel) to the ab plane. The dashed and solid lines indicate chain and ladder model fits, respectively. The inset to the upper panel shows the low temperature region for both orientations along with the high field behavior for $H_{\perp ab}$. The inset to the lower panel shows $M(H)$ of Ba_2CuTeO_6 for $H_{\perp ab}$.

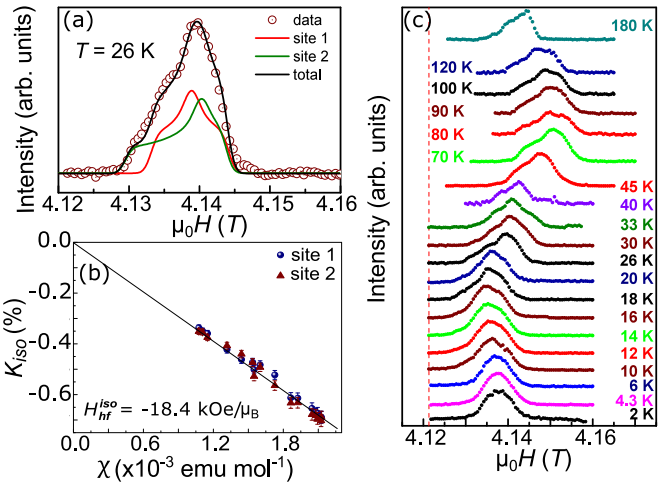

FIG. 3. (a) Fitting of experimental ^{125}Te NMR spectrum by simulation of the two Te crystallographic sites at 26 K [20]. (b) $K_{\rm iso}$ (%) vs $\chi(T)$ plots with the temperature as an implicit parameter for both Te sites. (c) Temperature dependence of ^{125}Te NMR spectra.

10^{-4} emu mol^{-1}, for $H_{\perp ab}$ gives $J/k_{\rm B} \approx 86$ K, $J'/J \approx 0.98$, and $g \approx 2.08$, with $\Delta/k_{\rm B} \approx 40$ K. At low temperatures $\chi(T)$ remains finite and deviates from ladder behavior as will be discussed later.

The ^{125}Te NMR data support the spin ladder picture discussed for the $\chi(T)$ data. The NMR spectrum of the powder sample consists of two components with a 1:1 ratio reflecting the two crystallographically inequivalent Te sites. Each spectrum is well characterized by a powder pattern with an anisotropic Knight shift tensor, as shown in Fig. 3(a) [20]. Above $T = 26$ K a linear relationship between $\chi(T)$ and $K(T)$ [see Fig. 3(b)] confirms that the observed $\chi(T)$ is an intrinsic property. The individual spectra are plotted in Fig. 3(c). These data are also shown in Fig. 4(a) as a color contour plot of the ^{125}Te NMR intensity in the temperature-magnetic field plane, with the dotted line as a guide to the eye, showing the

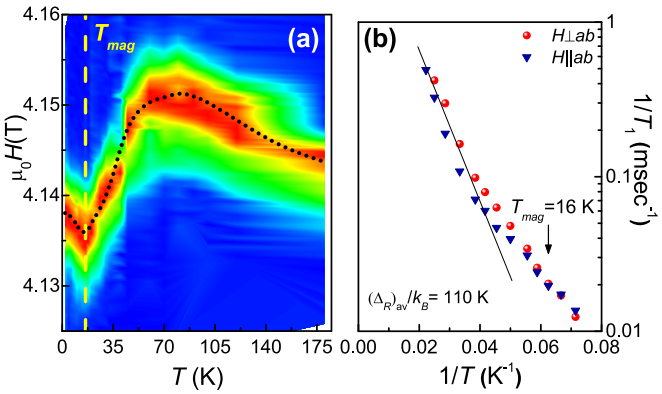

FIG. 4. (a) Contour plot of the spin echo intensity of the ^{125}Te-field-sweep NMR spectra as a function of temperature (NMR frequency: 55.44 MHz) for a polycrystalline sample. The dotted line is a guide to the eye. The individual spectra are plotted in Fig. 3(c). (b) Semilog plot of $1/T_1$ versus $1/T$. Solid lines correspond to the behavior $1/T_1 = A\exp(-\Delta_R/k_{\rm B}T)$ at high temperatures where Δ_R is the dynamical spin gap.

temperature dependence of the Knight shift $K(T)$. As shown in Fig. 4(b), the temperature dependence of the spin-lattice relaxation rate $1/T_1$ for $H_{\perp ab}$ and $H_{\parallel ab}$ in arrays of single crystals can be fitted by an Arrhenius type of behavior $[1/T_1 = A\exp(-\Delta_R/k_{\rm B}T)]$ in the range $50 \geqslant T \geqslant 25$ K with $\Delta_R/k_{\rm B} \approx 110$ K. The departure seen for $T \leqslant 25$ K may be due to the contribution from the interladder coupling as discussed below. The larger value of $\Delta_R/k_{\rm B}$ in comparison to $\Delta/k_{\rm B}$ from $\chi(T)$ is due to excitations from different wave vector components than those probed by $K(T)$ and $\chi(T)$. This effect has been well demonstrated both theoretically [21] and experimentally [22,23] and Δ_R therefore represents the dynamical spin gap. It should also be noted that no critical behavior, which would be expected if magnetic ordering occurs at around $T_{\rm mag} = 16$ K, is seen in $1/T_1$.

Estimates of effective exchange coupling constants from LSDA+U band structure calculations [24,25] support the previously described ladder picture. The total energy $E(\mathbf{q},\phi)$ was calculated as a function of a wave vector $\mathbf{q}$ and of an angle ϕ between spins of two Cu^{2+} ions in the $T = 300$ K monoclinic $C2/m$ unit cell for a number of spin-spiral structures. Effective exchange coupling constants were evaluated by fitting $E(\mathbf{q},\phi)$ to a classical Heisenberg model. We obtain antiferromagnetic leg coupling $J = 33.0$ meV and rung coupling $J' = 33.8$ meV for $U = 5$ eV, yielding almost isotropic $J'/J \approx 1.02$ in excellent agreement with the $\chi(T)$ fit. There is roughly a factor of 4 difference between J obtained experimentally and that from the $U = 5$ eV calculation. The calculated J parameters are found to scale down with increasing U approximately as $1/U$ and the agreement with the experimental values is not unreasonable given the uncertainties present. As expected, the other parameters are smaller than J and J'. The diagonal coupling j_1 is antiferromagnetic with $j_1/J \approx 0.05$. There are three main interladder couplings [see Figs. 1(b)–1(d)]. j_2 and j_3 are between ladders in the same plane (parallel to the ab plane), whereas j_4 couples ladders between planes through the face-shared TeO_6 octahedra [Figs. 1(b) and 1(c)]. j_2 and j_3 are ferromagnetic with $j_2/J \approx -0.06$ and $j_3/J \approx -0.05$ and have a frustrated two-bond geometry. The "interplane" coupling j_4 may be most important and is antiferromagnetic with $j_4/J \approx 0.03$. Calculations performed using the triclinic structure refined from high resolution neutron diffraction data collected at 1.8 K indicate that the main effect of the triclinic distortion is to reduce the frustration of the "intraplane" interladder interactions j_2 and j_3 with the coupling along the c axis direction remaining weak. These interladder couplings are small but not negligible, with a magnitude of the order of $0.1J$, which may potentially bring the system towards the QCP.

$\chi(T)$ deviates strongly from the expected ladder behavior below approximately $T^* \approx 25$ K, and at $T_{\rm mag} \approx 16$ K a cusp is seen below which the anisotropy of $\chi(T)$ becomes profound (inset to upper panel of Fig. 2). With lowering temperature below $T_{\rm mag} \approx 16$ K, $\chi_{\parallel ab}(T)$ shows a weak increase but in contrast $\chi_{\perp ab}(T)$ shows a decrease. Note that the upturn below $T_{\rm mag} \approx 16$ K for $\chi_{\parallel ab}(T)$ is reproduced by the temperature dependence of the ^{125}Te NMR intensity [Fig. 4(a)], confirming the intrinsic origin of this behavior [26]. The cusp is seen reproducibly in all batches of single crystals and all polycrystalline samples (see SM [20]). In the magnetization M-H curve (inset to lower panel of Fig. 2), a rapid increase,

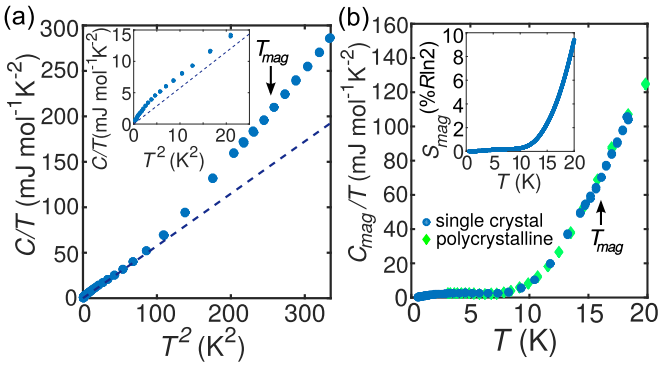

FIG. 5. (a) The specific heat C of single crystal Ba_2CuTeO_6 plotted as C/T vs T^2. The dashed line indicates an approximate lattice T^3 term as described in the text. The inset shows an enlarged view of the low temperature region. (b) The estimated magnetic specific heat $C_{\rm mag}(T)$ for Ba_2CuTeO_6 plotted as $C_{\rm mag}/T$ vs T. The inset shows the estimated magnetic entropy $S_{\rm mag}(T)$ as a percentage of $R\ln 2$ up to $T = 20$ K.

almost steplike, was observed around 1.5 T only for $H_{\perp ab}$. Since the behavior of $\chi(T)$ well above 1.5 T is quite similar to $\chi_{\parallel ab}(T)$, this anomaly likely represents a spin reorientation transition. All of these results point to the conclusion that the anomaly at $T_{\rm mag} \approx 16$ K is due to magnetic ordering. We argue that the ordering is associated with the small but finite interladder coupling and that the system has marginally passed the expected QCP. The deviation of $\chi(T)$ from ladder behavior at low temperatures could be understood as the manifestation of the effect of interladder coupling and quantum criticality.

A quantum Monte Carlo (QMC) simulation of $\chi(T)$ for isolated and coupled ladder systems [5] indicated very weak changes at high temperatures above $T^* = 0.2$–$0.3\ J/k_{\rm B}$ upon the introduction of the interladder coupling. At low temperatures below T^*, however, the thermally activated behavior of $\chi(T)$ reflecting the spin gap in the isolated system was found to be drastically suppressed by the interladder coupling. Eventually, passing the critical point, the thermally activated behavior is completely absent and a finite $T = 0$ susceptibility $\chi(0)$ emerges. Although the model used was too oversimplified to allow for quantitative comparison, the QMC result for coupled ladders above the critical point mimics the essential features of $\chi(T)$ in Ba_2CuTeO_6.

Despite the weak but clear signature of ordering at $T_{\rm mag}$ in $\chi(T)$, specific heat measurements in both zero field and applied fields of 5 and 13 T failed to find any clear anomaly indicative of ordering at $T_{\rm mag}$ (see Fig. 5(a) and SM [20]). Neutron diffraction experiments using a large-volume powder sample on Echidna at the OPAL reactor [27] showed no magnetic Bragg peaks [20], indicating a small ordered moment due to renormalization of the moment by quantum fluctuations. The upper bound for the moment expected to be detectable in the Echidna experiment is $\approx 0.5\ \mu_B$ and therefore further neutron diffraction investigations are underway to resolve the details of the ordering. Such strongly suppressed ordered magnetic moments in the vicinity of a quantum phase transition have been observed in other cases [11,28]. No anomaly in the NMR spin-lattice relaxation rate $1/T_1$ measured on aligned single crystals was detected upon passing through $T_{\rm mag}$ [Fig. 4(b)]. This absence of clear signals of long-range ordering indicates that the cusp seen in susceptibility is a "marginal" phase transition with weak signatures and a suppression of the ordered moment very likely due to quantum fluctuations [29].

The described lack of sharp specific heat anomaly at the marginal phase transition implies that the peak is smeared out by quantum critical fluctuations and indeed we detect indications of unquenched magnetic entropy at low temperatures. As seen in the inset to Fig. 5(a), C/T vs T^2 is not linear, even below 5 K. A best estimate of the phononic T^3 lattice contribution, from fitting $C/T = \beta T^2$ below $T = 8.5$ K, is indicated as a dashed line in Fig. 5(a). For the nonmagnetic analog Ba_2ZnTeO_6, C/T vs T^2 is completely linear below 5 K [30] and the Debye temperature of Ba_2CuTeO_6 ($\theta_D \approx 323$ K), estimated from the dashed line in Fig. 5(a), agrees reasonably well with that of Ba_2ZnTeO_6 ($\theta_D \approx 377$ K). These facts indicate that the dashed line in Fig. 5(a) is a reasonable estimate of the lattice contribution and that there is an additional contribution to the specific heat other than the lattice which can naturally be ascribed to $S = \frac{1}{2}$ spins. The magnetic specific heat $C_{\rm mag}(T)$ was estimated by subtracting the aforementioned phononic T^3 term from the total specific heat, the result is shown in Fig. 5(b). $C_{\rm mag}(T)$ was then integrated to provide an estimate of the magnetic entropy $S_{\rm mag}(T)$, shown in the inset to Fig. 5(b), which is approximately 4.5% of $R\ln 2$ at 17 K. Despite the presence of such a large magnetic entropy at low temperature, no clear anomaly is present in $C_{\rm mag}(T)$ at $T_{\rm mag} \approx 16$ K and the entropy is quenched only gradually to $T = 0$ K. We argue that the large magnetic specific heat observed around $T_{\rm mag} \approx 16$ K represents the quantum fluctuations associated with the close proximity to the QCP.

After submission of our manuscript another paper reporting the physical properties of Ba_2CuTeO_6 was published by Rao *et al.* [31]. Rao *et al.* identify the same features as we do in susceptibility, also see the weak transition at $H \approx 1.5$ T in $M(H)$ and also fail to detect a sharp anomaly in zero field specific heat although they do see an extremely weak hump in the vicinity of $T_{\rm mag}$. That our independent studies determine the same features is further confirmation of their intrinsic nature. Despite the experimental consistency, the theoretical exchange path analysis of Rao *et al.* does differ from ours substantially. They identify ladders in their triclinic ac plane based upon the room temperature structure refined using a triclinic model from room temperature synchrotron data. The origin of the conflict between our results remains to be resolved but perhaps the one potential source is the structural data used for input. Our calculations are based upon structures refined from high resolution neutron diffraction which is intrinsically much more sensitive to oxygen positions, especially in the presence of heavy elements such as Ba and Te. The consistency between our room temperature monoclinic and low temperature triclinic calculations confirms that the interactions are not substantially changed by the triclinic distortion, consistent with their orbital ordering origin.

We will now set Ba_2CuTeO_6 in the context of other spin-ladder and quasi-1D systems with magnetic order. Previous examples in the literature of ordering in $S = \frac{1}{2}$ ladders or chains have involved clear signatures such as sharp anomalies in heat capacity [11,32–34] and divergent peaks in NMR $1/T_1$ [35,36]. In ladder materials with field-induced magnetic

ordering the onset of long-range order is also usually unambiguous [37,38]. The behavior of Ba_2CuTeO_6 is therefore, to the best of our knowledge, in clear contrast to other similar systems. The lack of an anomaly in $1/T_1$ is the most unusual feature. $1/T_1$ is generally a very reliable probe of ordering in low-dimensional systems [35,36,39,40]. There are cases in which a change in gradient or cusp rather than a divergent peak is seen in $1/T_1$ in low-dimensional quantum magnets [28]. This is thought to be related to the suppression of classical antiferromagnetic ordering by quantum fluctuations, as we propose to be the case in Ba_2CuTeO_6. The origin of the lack of any divergent peak or increase in $1/T_1$ around the ordering temperature T_{mag} in Ba_2CuTeO_6, along with the precise nature of the ordering, remains unclear and further experimental and theoretical investigations are required. The small ordered moment and weak signatures of the transition point to the influence of quantum fluctuations due to the proximity to the QCP.

In conclusion, we have discovered that Ba_2CuTeO_6 is a clean, site ordered system with "hidden" antiferromagnetic $S = \frac{1}{2}$ spin ladders due to ferro-orbital ordering on the Cu^{2+} site. The very weak signature of order in $\chi(T)$, without any corresponding clear signature of long-range order yet detected in specific heat, neutron diffraction, or NMR points to the conclusion that Ba_2CuTeO_6 is almost precisely at the QCP for the antiferromagnetic $S = \frac{1}{2}$ weakly coupled ladder system, where quantum fluctuations dominate. Compared to other systems close to the QCP, such as (Dimethylammonium)(3,5-dimethylpyridinium)$CuBr_4$, in which clear thermodynamic signatures of order are seen, Ba_2CuTeO_6 may provide a better opportunity to study the quantum criticality of the weakly coupled ladder system.

The authors thank Jérôme Dufour, George Jackeli, Frédéric Mila, Masaaki Nakamura, Seiji Niitaka, and Andreas W. Rost for invaluable discussions. A.S.G. thanks Professor A. P. Mackenzie and Professor P. Lightfoot for support in the early stages of the project. This work was partly supported by Grant-in-Aid for Scientific Research (S) (Grant No. 24224010) and the Alexander von Humboldt Stiftung.

[1] T. Barnes, E. Dagotto, J. Riera, and E. S. Swanson, Phys. Rev. B **47**, 3196 (1993).
[2] B. Normand and T. M. Rice, Phys. Rev. B **54**, 7180 (1996).
[3] M. Troyer, M. E. Zhitomirsky, and K. Ueda, Phys. Rev. B **55**, R6117(R) (1997).
[4] M. Imada and Y. Iino, J. Phys. Soc. Jpn. **66**, 568 (1997).
[5] D. C. Johnston, M. Troyer, S. Miyahara, D. Lidsky, K. Ueda, M. Azuma, Z. Hiroi, M. Takano, M. Isobe, Y. Ueda, M. A. Korotin, V. I. Anisimov, A. V. Mahajan, and L. L. Miller, arXiv:cond-mat/0001147.
[6] A. Shapiro, C. P. Landee, M. M. Turnbull, J. Jornet, M. Deumal, J. J. Novoa, M. A. Robb, and W. Lewis, J. Am. Chem. Soc. **129**, 952 (2007).
[7] B. Thielemann, C. Rüegg, K. Kiefer, H. M. Rønnow, B. Normand, P. Bouillot, C. Kollath, E. Orignac, R. Citro, T. Giamarchi, A. M. Läuchli, D. Biner, K. W. Krämer, F. Wolff-Fabris, V. S. Zapf, M. Jaime, J. Stahn, N. B. Christensen, B. Grenier, D. F. McMorrow, and J. Mesot, Phys. Rev. B **79**, 020408 (2009).
[8] M. A. Korotin, V. I. Anisimov, T. Saha-Dasgupta, and I. Dasgupta, J. Phys.: Condens. Matter **12**, 113 (2000).
[9] T. Ohama, M. Isobe, and Y. Ueda, J. Phys. Soc. Jpn. **70**, 1801 (2001).
[10] F. Awwadi, R. D. Willett, B. Twamley, R. Schneider, and C. P. Landee, Inorg. Chem. **47**, 9327 (2008).
[11] T. Hong, K. P. Schmidt, K. Coester, F. F. Awwadi, M. M. Turnbull, Y. Qiu, J. A. Rodriguez-Rivera, M. Zhu, X. Ke, C. P. Aoyama, Y. Takano, H. Cao, W. Tian, J. Ma, R. Custelcean, H. D. Zhou, and M. Matsuda, Phys. Rev. B **89**, 174432 (2014).
[12] P. Köhl and D. Reinen, Z. Anorg. Allg. Chem. **409**, 257 (1974).
[13] We note that high resolution neutron diffraction on HRPD at ISIS showed the presence of a very weak transition from $C2/m$ to $P\bar{1}$ symmetry at $T = 287$ K. The details will be reported elsewhere [A. S. Gibbs, K. S. Knight, P. J. Saines, J. R. Hester and H. Takagi (unpublished)].
[14] D. Khomskii, *Transition Metal Compounds* (Cambridge University Press, Cambridge, 2014).
[15] R. M. Ibberson, W. I. F. David, and K. S. Knight, Rutherford Appleton Laboratory Report No. RAL-92031 (1992).
[16] R. M. Ibberson, Nucl. Instrum. Methods Phys. Res. Sect. A **600**, 47 (2009).
[17] P. Köhl, U. Müller, and D. Reinen, Z. Anorg. Allg. Chem. **392**, 124 (1972).
[18] J. C. Bonner and M. E. Fisher, Phys. Rev. **135**, A640 (1964).
[19] W. E. Hatfield, R. R. Weller, and J. W. Hall, Inorg. Chem. **19**, 3825 (1980).
[20] See Supplemental Material at http://link.aps.org/supplemental/10.1103/PhysRevB.95.104428 for further details of structural determination, susceptibility, NMR, and high field measurements and electronic structure calculations.
[21] J. Kishine and H. Fukuyama, J. Phys. Soc. Jpn. **66**, 26 (1997).
[22] Y. Itoh and H. Yasuoka, J. Phys. Soc. Jpn. **66**, 334 (1997).
[23] G. Chaboussant, M.-H. Julien, Y. Fagot-Revurat, L. P. Lévy, C. Berthier, M. Horvatić, and O. Piovesana, Phys. Rev. Lett. **79**, 925 (1997).
[24] A. I. Liechtenstein, V. I. Anisimov, and J. Zaanen, Phys. Rev. B **52**, R5467(R) (1995).
[25] A. N. Yaresko, V. N. Antonov, and P. Fulde, Phys. Rev. B **67**, 155103 (2003).
[26] The NMR data were taken at a frequency of 55.44 MHz, corresponding to a magnetic field of 4.12 T and in this high field region the susceptibility for $H_{\perp ab}$ also increases below T_{mag} therefore the polycrystalline samples show an increase in $\chi(T)$ below T_{mag} at this field since both $\chi(H_{\parallel ab})$ and $\chi(H_{\perp ab})$ increase below T_{mag}.
[27] K.-D. Liss, B. Hunter, M. Hagen, T. Noakes, and S. Kennedy, Phys. B **385-386**, 1010 (2006).
[28] M. Yoshida, Y. Okamoto, M. Takigawa, and Z. Hiroi, J. Phys. Soc. Jpn. **82**, 013702 (2013).
[29] P. Mendels and F. Bert, C. R. Phys. **17**, 455 (2016).
[30] Ba_2ZnTeO_6 has a higher symmetry structure than Ba_2CuTeO_6 in the low temperature regime (with space group $C2/m$ compared to the $P\bar{1}$ space group of Ba_2CuTeO_6 in this range [13]) and can therefore not be used for a reliable subtraction. However, the

similar Debye temperature indicates that our estimated T^3 term is reasonable.

[31] G. N. Rao, R. Sankar, A. Singh, I. P. Muthuselvam, W. T. Chen, V. N. Singh, G.-Y. Guo, and F. C. Chou, Phys. Rev. B **93**, 104401 (2016).

[32] V. N. Glazkov, G. Dhalenne, A. Revcolevschi, and A. Zheludev, J. Phys.: Condens. Matter **23**, 086003 (2011).

[33] B. Roessli, U. Staub, A. Amato, D. Herlach, P. Pattison, K. Sablina, and G. A. Petrakovskii, Physica B **296**, 306 (2001).

[34] G. Deng, M. Kenzelmann, S. Danilkin, A. J. Studer, V. Pomjakushin, P. Imperia, E. Pomjakushina, and K. Conder, Phys. Rev. B **88**, 174424 (2013).

[35] F. Casola, Ph.D. thesis, ETH Zurich, 2013.

[36] S. Matsumoto, Y. Kitaoka, K. Ishida, K. Asayama, Z. Hiroi, N. Kobayashi, and M. Takano, Phys. Rev. B **53**, R11942 (1996).

[37] Z. Honda, H. Aruga Katori, M. Ikeda, M. Hagiwara, K. Okunishi, M. Sakai, T. Fukuda, and N. Kamata, J. Phys. Soc. Jpn. **81**, 113710 (2012).

[38] P. R. Hammar, D. H. Reich, C. Broholm, and F. Trouw, Phys. Rev. B **57**, 7846 (1998).

[39] H. Yoshida, Y. Okamoto, T. Tayama, T. Sakakibara, M. Tokunaga, A. Matsuo, Y. Narumi, K. Kindo, M. Yoshida, M. Takigawa, and Z. Hiroi, J. Phys. Soc. Jpn. **78**, 043704 (2009).

[40] F. Bert, D. Bono, P. Mendels, F. Ladieu, F. Duc, J.-C. Trombe, and P. Millet, Phys. Rev. Lett. **95**, 087203 (2005).